

Submitted to Ap J L

Gas Density, Stability and Starbursts Near the Inner Lindblad Resonance of the Milky Way

Antony A. Stark, Christopher L. Martin, Wilfred M. Walsh, Kecheng Xiao, Adair P. Lane

Harvard-Smithsonian Center for Astrophysics, 60 Garden St., Cambridge MA 02138

aas@cfa.harvard.edu

and

Christopher K. Walker

Steward Observatory, University of Arizona, Tucson, AZ 85721

cwalker@as.arizona.edu

ABSTRACT

A key project of the Antarctic Submillimeter Telescope and Remote Observatory reported by Martin et al. (2004) is the mapping of CO $J = 4 \rightarrow 3$ and $J = 7 \rightarrow 6$ emission from the inner Milky Way, allowing determination of gas density and temperature. Galactic center gas that Binney et al. (1991) identify as being on x_2 orbits has a density near $10^{3.5} \text{ cm}^{-3}$, which renders it only marginally stable against gravitational coagulation into a few Giant Molecular Clouds, as discussed by Elmegreen (1994). This suggests a relaxation oscillator mechanism for starbursts in the Milky Way, where inflowing gas accumulates in a ring at 150 pc radius for approximately 20 million years, until the critical density is reached, and the resulting instability leads to the sudden formation of giant clouds and the deposition of $4 \times 10^7 M_\odot$ of gas onto the Galactic center.

Subject headings: Galaxy: structure—ISM: clouds—ISM: molecules—galaxies: starburst—stars:formation

1. Introduction

Dynamics of gas in the inner few kiloparsecs of the Milky Way are dominated by the non-axisymmetric gravitational potential of the central bar. The properties of this bar are now well known, and there is good agreement between observations of gas motion and model fits to the potential (Jenkins & Binney 1994; Gerhard 1999; Häfner et al. 2000; Bissantz et al. 2003). As suggested by Binney et al. (1991), the gas tends to be found on families of closed orbits which are not self-intersecting. All non-closed orbits and some closed orbits are self-intersecting. Gas on such orbits will shock and lose energy where the gas streamlines intersect, and the gas will then move inwards to a lower energy orbit. If the gas can find its way onto a family of non-self-intersecting closed orbits, the energy dissipation slows and the timescale for orbital changes lengthens out. Contopoulos & Mertzaniades (1977) described two families of closed orbits in barred galaxies: the “ x_1 ”, which are elongated along the bar and found outside the inner Lindblad resonance (ILR); and the “ x_2 ”, which are more round and can be found near the ILR and inside it. The ILR is located where the epicyclic frequency of a particle orbiting in the Galactic potential resonates with the pattern speed of the bar. This occurs at a radius of approximately 450 pc from the center of the Milky Way (Bissantz et al. 2003).

Gas which is several kiloparsecs away from the Galactic center tends to be driven inwards until it reaches a region within a few hundred parsecs of the ILR, because the interaction of the bar potential with the gas exerts a negative torque, resulting in loss of angular momentum by the gas (Lynden-Bell & Kalnajs 1972; Athanassoula 1988; Jenkins & Binney 1994). Near the ILR this effect disappears, because the net torque there is small or zero, and inwards of the ILR it may even reverse and become positive, so that gas inside the ILR could be driven outwards (Combes 1988). Gas therefore accumulates in a ring near the ILR. Unlike the gas further out, the dynamics of this gas depends critically on its self gravity (Elmegreen 1994; Jenkins & Binney 1994), and therefore on its thermodynamic properties, density in particular.

The thermodynamic properties of the gas can be determined by millimeter- and sub-millimeter-wave spectral line observations. The distribution of molecular gas near the ILR is known from extensive surveys in CO and ^{13}CO $J = 1 \rightarrow 0$ and $J = 2 \rightarrow 1$ (Bally et al. 1988; Bitran et al. 1997; Oka et al. 1998); these spectral lines show the presence of molecular gas. These lines alone do not, however, determine its density or excitation temperature. Observations of the mid- J lines of CO provide the missing information. Since the low- J states of CO are in local thermodynamic equilibrium (LTE) in almost all molecular gas (Goldreich & Kwan 1974), measurements of mid- J states are critical to achieving a solution of the radiative transfer by breaking the degeneracy between beam filling factor and

excitation temperature. A new survey (Martin et al. 2004) by the Antarctic Submillimeter Telescope and Remote Observatory (AST/RO, Stark et al. 2001) adds the $J = 4 \rightarrow 3$ (461 GHz) and $J = 7 \rightarrow 6$ (807 GHz) rotational lines of CO to existing lower-frequency data (Bally et al. 1988). These data are available on the AST/RO website¹ for general use. These measurements have recently been modeled using the large velocity gradient (LVG) approximation to determine the gas density and temperature.

In this *Letter*, we discuss the implications of the Martin et al. (2004) density estimates for Galactic center gas. We apply our new data, specific to the Milky Way, to the general analysis of stability of dense gas near ILR regions in galaxies by Elmegreen (1994). We find that the gas near 150 pc radius is marginally unstable. This suggests that in the past there has been a period of stability and gas build-up. In the future, the instability will create a few giant clouds, resulting in a starburst and the deposition of tens of millions of solar masses of material on the Galactic center. This process repeats with a cycle time determined by the rate at which gas precipitates on the Galactic center region from outside, resulting in starbursts at intervals of approximately 20 million years.

2. Gas Density

Figure 1 is a representation of the average density of the molecular gas layer in the vicinity of the ILR. Martin et al. (2004) used an LVG model on their survey data to estimate the density and temperature at each point in (ℓ, b, v) . Density values in Figure 1 are calculated by averaging the logarithm of the density values from Martin et al. (2004) at each value of (ℓ, v) , as b varies from -0.3 to 0.2 , excluding points where the LVG fit is uncertain. The excluded points are those where the average $^{12}\text{CO } J = 1 \rightarrow 0$ emission in Bally et al. (1988) is less than 0.2K , or where the average density is below $10^{2.5} \text{cm}^{-3}$, which is an approximate lower limit to the validity of the Martin et al. (2004) LVG model. The pixels at some values of (ℓ, v) in Figure 1 appear white, and this can be for several reasons: (1) there are no data at that position since the survey is limited in v by the bandwidth of the spectrometer; (2) there is no significant CO emission; (3) the density is below the threshold of validity of the model; (4) the variance in the average over b exceeds $(10^3 \text{cm}^{-3})^2$. The model has converged to a consistent value at the points where a density is displayed. Even those values could be spurious if the assumptions used in the LVG approximation do not apply. This certainly occurs where there is foreground absorption far from the emitting region, for example between -60 and $+25 \text{km s}^{-1}$, where spiral arms in the Galactic disk are

¹<http://cfa-www.harvard.edu/ASTRO>

projected onto the Galactic center emission. This region is hatched in Figure 1.

Superposed on the data are some closed orbits from the model of Bissantz et al. (2003). The cusped x_1 orbit and two self-intersecting x_1 orbits are shown in magenta. The cusped x_1 orbit is the innermost x_1 orbit which does not self-intersect, with an apogee 1300 pc from the Galactic center. The two self-intersecting x_1 orbits are interior to this, with apogees near 1000 pc. The x_2 orbits begin inside the ILR, and are drawn in brown. The outermost x_2 has an apogee of 180 pc. The x_2 orbits extend all the way into the Galactic center; the innermost shown here is almost circular and has an apogee of 23 pc. These same orbits are plotted differently in Figures 10 and 11 of Bissantz et al. (2003).

We see that in some places along the cusped x_1 orbit, $n(\text{H}_2) \approx 10^3$ to 10^4 cm^{-3} , although the gas is clumpy and the average density on this orbit is less. Most places along the outer x_2 orbit have $n(\text{H}_2) \approx 2 \times 10^3$ to $6 \times 10^3 \text{ cm}^{-3}$, with few values outside this range. The densities on the x_2 orbits which are at negative ℓ and negative v are unreliable, because these parts of the orbit lie about 1 kpc behind some of the outer x_1 orbits (not shown in Figure 1) which have the same velocity but lower excitation. Most of the region between the cusped x_1 orbit and the outermost x_2 orbit has lower density and little molecular emission.

3. Gas Stability

Given a measure of the gas density on orbits near the ILR, it is possible to determine whether or not that gas is stable—if the gas is sufficiently dense, its self-gravity will overcome the tidal shear of the Galaxy’s gravitational potential and it will agglomerate into clouds. The dynamics of this situation has been analyzed by Elmegreen (1994), who linearized the hydromagnetic force and continuity equations in a rotating frame and thereby derived a dispersion relation for the growth of instabilities in a gas ring near the ILR. He determined that the growth rate is a function of gas density and pressure, the Galactic potential, magnetic field strength, and the rate at which material accretes from larger radii. This relation is expressed in equation 11 of Elmegreen (1994):

$$\omega_r^2 - \omega_G^2 + \Omega_a \omega_r + \frac{\kappa^2 \omega_r^2}{\omega_r^2 + k^2 v_A^2 + \Omega_a \omega_r} \approx 0, \quad (1)$$

where ω_r is the growth rate of instability, k is its wavenumber, κ is the epicyclic frequency in the Galactic potential, v_A is the Alfvén velocity corresponding to the azimuthal magnetic field, Ω_a is the relative accretion rate, and ω_G is a frequency related to the acceleration of self-gravity. Values of the quantities in Equation 1 are estimated in Table 1.

The relative accretion rate, Ω_a , is a measure of gas inflow from larger radii. It is

determined by processes outside the ILR region: the amount of gas in the outer regions of the bar, and the torques exerted on that gas by the bar. At minimum, the evolved stars in the bulge will eject matter into the interstellar medium of the outer bar at a rate $\sim 0.2 M_{\odot} \text{yr}^{-1}$ (Jungwiert et al. 2001). At maximum, the Galactic center region could ingest an entire gas-rich dwarf companion at a rate of 100 to 1000 $M_{\odot} \text{yr}^{-1}$. Accretion rates higher than this would disrupt the inner Galaxy, so we can conclude they have not occurred in the Milky Way (Heller & Shlosman 1994; Bournaud & Combes 2002). Combes (2004) suggests an accretion rate of $10 M_{\odot} \text{yr}^{-1}$, which is approximately the rate of accretion of intergalactic material onto the Galaxy. This rate, accreting onto inner gas disk of $\sim 2 \times 10^8 M_{\odot}$, yields $\Omega_a \sim 50 \text{Gyr}^{-1}$.

There is as yet no measurement of the strength of the magnetic field in the dense Galactic center gas, although the existence of a magnetic field perpendicular to the disk near the Galactic center is demonstrated by the non-thermal radio filaments (Yusef-Zadeh et al. 1984), and the existence of a magnetic field in the plane of the disk is demonstrated by submillimeter-wave polarimetry (Novak et al. 2003). Chuss et al. (2003) have estimated the field strength to be about a milliGauss, based on the field morphology. The perpendicular field near the center, they argue, is the result of a process where the field in the disk is amplified until the magnetic field pressure begins to dominate the dynamics and the field decouples from the gas in the regions of relative lower density. This implies that the magnetic field energy in the regions of relative higher density self-regulates to approximate equipartition with the internal kinetic energy of the gas, making the Alfvén velocity, v_A , comparable to the internal turbulent velocity of the molecular gas. Accepting this argument leads to a value of v_A in Equation 1 which is significant but not dominant. In other barred galaxies, the observed field strength averaged over the central few kiloparsecs is typically $10 \mu\text{G}$ (Beck et al. 2002). Since the dense gas has a filling factor of $\sim 10^{-2}$, this is consistent with a milliGauss field in the dense gas.

The epicyclic frequency, κ , is more certain. It depends only on the rotation curve and its derivative, which are known within $\pm 20\%$. In Table 1 we adopt values taken from Figure 1 of Bissantz et al. (2003).

Elmegreen (1991) approximates the equation of state for the molecular gas as $\Delta P \approx \gamma_{\text{eff}} c^2 \Delta \rho$, where the complexities of heating and cooling of the molecular gas are subsumed in an effective ratio of specific heats $\gamma_{\text{eff}} \sim 0.3$ to 2, and an effective sound speed $c \sim 10$ to 40km s^{-1} . As pointed out in Elmegreen (1994), the quantity $\gamma_{\text{eff}} c^2$ for the actual gas under analysis can be estimated by considering the equilibrium between pressure and self-gravity perpendicular to the plane: $h \approx (2/e) \gamma_{\text{eff}}^{1/2} c \kappa^{-1}$, where the scaleheight, h , is determined from observations. Applied to the values in Table 1, this procedure gives $\gamma_{\text{eff}} \gtrsim 1$ if $c \sim v_A \sim$

25 km s⁻¹.

The gravitational frequency, ω_G , as defined by Elmegreen (1994) is a measure of the relative importance of self-gravity compared to pressure in the gas over a scalelength given by wavenumber k :

$$\omega_G \approx 2 G\mu k^2 \ln\left(\frac{2}{kh}\right) - k^2 \gamma_{\text{eff}} c^2 \quad (2)$$

where $\mu = \rho\pi h^2$ is the mass per unit length in the ring. The ω_G has a maximum when $k_{\text{max}} \approx 2h^{-1} \exp[-0.5(1 + \gamma_{\text{eff}} c^2 / G\mu)]$, and the corresponding gravitational frequency, $\omega_G = G\mu k_{\text{max}}^2$ corresponds to the fastest growing unstable mode.

We are now in a position to evaluate ω_r , the growth rate of the fastest unstable mode, by substituting k_{max} for k . Equation 1 is quartic in ω_r with one positive real solution. If $\Omega_a \ll \kappa$, and $k_{\text{max}} v_A \lesssim \kappa$, as we see is the case from Table 1, then

$$\begin{aligned} \omega_r &\ll \omega_G && \text{if } \omega_G \ll \kappa, \text{ and} \\ \omega_r &\approx \omega_G && \text{if } \omega_G \gtrsim \kappa. \end{aligned}$$

In the Milky Way at the present time, the accretion term Ω_a is not dynamically significant to the instability (although it does determine the time *between* instabilities), and the magnetic field term v_A has only marginal significance, since its contribution to the dynamics is in approximate equipartition with the other terms. The growth rate of the instability is small as long as $\omega_G \ll \kappa$, but becomes significant when $\omega_G \sim \kappa$. The dominant dynamical effect is the competition between the tidal shear of the Galaxy and the tendency for the gas ring to clump with wavelength $\lambda_{\text{max}} = 2\pi/k_{\text{max}}$. The criterion for significant instability, $\omega_G > \kappa$, can be expressed as a threshold in gas density:

$$n(\text{H}_2) > n_{\text{crit}}(\text{H}_2) \approx \frac{0.2\kappa^2}{Gm_{\text{H}}} \approx 10^{3.5} \left[\frac{\kappa}{1000 \text{ Gyr}^{-1}} \right]^2, \quad (3)$$

which is essentially a density criterion for the formation of molecular clouds in the presence of Galactic tidal forces (Stark et al. 1989). The region that begins to contract will initially have a mass approximately equal to $\mu_{\text{max}} \lambda_{\text{max}} = 4 \times 10^7 M_{\odot}$. As the instability proceeds, the dynamics will become non-linear, and move beyond the valid regime of Equation 1. This merits further study.

4. Starbursts in the Milky Way

We see from Figure 1 that gas on the inner x_1 orbits exceeds the critical density threshold in places, and that the gas is clumped. The gas on the outer x_2 orbits is more smooth, but

is at the threshold of significant instability. The timescale for clumping to begin is short: $1/\omega_r \sim 1 \text{ Myr}$. Since $\lambda_{\text{max}} \approx r$, we expect the instability to result in only a few large clouds, containing many millions of solar masses. The Giant Molecular Cloud surrounding Sgr B2, which can be seen as a relatively minor density enhancement in Figure 1 at $\ell = 0.65^\circ$, $v = 60 \text{ km s}^{-1}$, is such a cloud. Because of their large mass, these clouds are subject to dynamical friction with the background of stars in the Galactic bulge, and will spiral into the center within 1 Gyr (Stark et al. 1991). Dynamical friction can overcome the forces tending to maintain the gas in the ILR region, and allow the gas to continue inwards toward the galactic center, but only if the gas is organized into sufficiently large self-gravitating clouds. This suggests a relaxation oscillator mechanism for quasi-periodic starbursts in the center of the Milky Way. At first, the Galactic center region is relatively clear of gas, like the central region of M31 is now. Gas precipitates into the region of the bar, either as mass loss from evolved stars or as the result of cannibalism of smaller galaxies. The bar dynamics drive this gas toward the ILR, where it will tend to accumulate in a ring as long as $n(\text{H}_2) \ll n_{\text{crit}}$. The ring becomes more and more dense as gas continues to precipitate from larger radii, and eventually the threshold is reached. A few giant clouds will form on a relatively short timescale, creating a starburst, and the giant clouds will be swept toward the center by dynamical friction, restoring a condition of relatively low density. The cycle will repeat on timescales of $\Omega_a^{-1} \sim 20 \text{ Myr}$, but of course this timescale is highly variable and can be dramatically shortened by events which precipitate a large amount of gas.

Support was provided by NSF grant OPP-0126090. We thank our AST/RO colleagues Richard Chamberlin, Jacob Kooi, and Gregory Wright for extensive help with the instrumentation.

REFERENCES

- Athanassoula, E. 1988, in Proceedings of the joint Varenna-Abastumani International School & Workshop on Plasma Physics, ed. T. D. Guyenne & J. J. Hunt, Vol. I (ESA SP-285), 341
- Bally, J., Stark, A. A., Wilson, R. W., & Henkel, C. 1988, *ApJ*, 324, 223
- Beck, R., Shoutenkov, V., Ehle, M., Harnett, J. I., Haynes, R. F., Shukurov, A., Sokoloff, D. D., & Thierbach, M. 2002, *A&A*, 391, 83
- Binney, J., Gerhard, O. E., Stark, A. A., Bally, J., & Uchida, K. I. 1991, *MNRAS*, 252, 210
- Bissantz, N., Englmaier, P., & Gerhard, O. 2003, *MNRAS*, 340, 949

- Bitran, M., Alvarez, H., Bronfman, L., May, J., & Thaddeus, P. 1997, *A&AS*, 125, 99
- Bournaud, F. & Combes, F. 2002, *A&A*, 392, 83
- Chuss, D. T., Davidson, J. A., Dotson, J. L., Dowell, C. D., Hildebrand, R. H., Novak, G., & Vaillancourt, J. E. 2003, *ApJ*, 599, 1116
- Combes, F. 1988, in *Galactic and Extragalactic Star Formation*, ed. R. E. Pudritz & M. Fich (Kluwer), 475
- Combes, F. 2004, in *The Interplay among Black Holes, Stars and ISM in Galactic Nuclei*, Proc. IAU Symposium 222, ed. T. S. Bergmann, L. C. Ho, & H. R. Schmitt, [astro-ph/0404210](#)
- Contopoulos, G. & Mertzaniades, C. 1977, *A&A*, 61, 477
- Elmegreen, B. G. 1991, *ApJ*, 378, 139
- . 1994, *ApJ*, 425, L73
- Gerhard, O. E. 1999, in *ASP Conf. Ser. 182: Galaxy Dynamics - A Rutgers Symposium*, 307
- Goldreich, P. & Kwan, J. 1974, *ApJ*, 189, 441
- Häfner, R., Evans, N. W., Dehnen, W., & Binney, J. 2000, *MNRAS*, 314, 433
- Heller, C. H. & Shlosman, I. 1994, *ApJ*, 424, 84
- Jenkins, A. & Binney, J. 1994, *MNRAS*, 270, 703
- Jungwiert, B., Combes, F., & Palouš, J. 2001, *A&A*, 376, 85
- Lynden-Bell, D. & Kalnajs, A. J. 1972, *MNRAS*, 157, 1
- Martin, C. L., Walsh, W. M., Xiao, K., Lane, A. P., Walker, C. K., & Stark, A. A. 2004, *ApJS*, 150, 239
- Novak, G., Chuss, D. T., Renbarger, T., Griffin, G. S., Newcomb, M. G., Peterson, J. B., Loewenstein, R. F., Pernic, D., & Dotson, J. L. 2003, *ApJ*, 583, L83
- Oka, T., Hasegawa, T., Sato, F., Tsuboi, M., & Miyazaki, A. 1998, *ApJS*, 118, 455

Stark, A. A., Bally, J., Balm, S. P., Bania, T. M., Bolatto, A. D., Chamberlin, R. A., Engargiola, G., Huang, M., Ingalls, J. G., Jacobs, K., Jackson, J. M., Kooi, J. W., Lane, A. P., Lo, K.-Y., Marks, R. D., Martin, C. L., Mumma, D., Ojha, R., Schieder, R., Staguhn, J., Stutzki, J., Walker, C. K., Wilson, R. W., Wright, G. A., Zhang, X., Zimmermann, P., & Zimmermann, R. 2001, *PASP*, 113, 567

Stark, A. A., Bally, J., Wilson, R. W., & Pound, M. W. 1989, in *The Center of the Galaxy*, ed. M. Morris (Leiden: Dordrecht), 129–133

Stark, A. A., Gerhard, O. E., Binney, J. J., & Bally, J. 1991, *MNRAS*, 248, 14p

Yusef-Zadeh, F., Morris, M., & Chance, D. 1984, *Nature*, 310, 557

Table 1. Quantities relating to the stability of gas near the ILR.

Quantity		Value at $r = 150$ pc	Value at $r = 450$ pc	Accuracy	Reference
Max. molecular number density	$n_{\max}(\text{H}_2)$	$6 \times 10^3 \text{ cm}^{-3}$	10^4 cm^{-3}	A	Martin et al. (2004)
Max. gas density	$\rho_{\max} = 2.4 \cdot m_{\text{H}} \cdot n_{\max}(\text{H}_2)$	$178 \text{ M}_{\odot} \text{ pc}^{-3}$	$296 \text{ M}_{\odot} \text{ pc}^{-3}$	A	
Relative accretion rate	Ω_a	50 Gyr^{-1}	50 Gyr^{-1}	C	Combes (2004)
Azimuthal magnetic field	B_{θ}	1 mG	1 mG	C	Chuss et al. (2003)
Az. Alfvén velocity	$v_A = B_{\theta}(4\pi\rho_{\max})^{-1/2}$	26 km s^{-1}	20 km s^{-1}	C	
Galactic angular velocity	Ω	620 Gyr^{-1}	314 Gyr^{-1}	A	Bissantz et al. (2003)
Derivative of Ω	$d\Omega/dr$	$-2500 \text{ Gyr}^{-1} \text{ kpc}^{-1}$	$-490 \text{ Gyr}^{-1} \text{ kpc}^{-1}$	A	Bissantz et al. (2003)
Epicyclic frequency	$\kappa = (4\Omega^2 + 2r\Omega d\Omega/dr)^{1/2}$	1036 Gyr^{-1}	506 Gyr^{-1}	A	
Molecular half-scaleheight	h	21 pc	56 pc	A	Bally et al. (1988)
Ratio of specific heats	$\gamma_{\text{eff}}c^2 \equiv \Delta P/\Delta\rho \approx (h\kappa c)^2/4$	$874 \text{ km}^2 \text{ s}^{-2}$	$1483 \text{ km}^2 \text{ s}^{-2}$	B	Elmegreen (1991)
Max. mass per length of ring	$\mu_{\max} = \pi\rho_{\max}h^2$	$2.5 \times 10^8 \text{ M}_{\odot} \text{ kpc}^{-1}$	$2.8 \times 10^9 \text{ M}_{\odot} \text{ kpc}^{-1}$	B	Elmegreen (1994)
Wavenumber of max. growth	$k_{\max} \approx 2h^{-1}\exp[-0.5(1 + \gamma_{\text{eff}}c^2/G\mu_{\max})]$	38 kpc^{-1}	20 kpc^{-1}	B	Elmegreen (1994)
Wavelength of max. growth	$\lambda_{\max} = 2\pi/k_{\max}$	165 pc	314 pc	B	Elmegreen (1994)
Gravitational frequency at k_{\max}	$\omega_G = k_{\max}(G\mu_{\max})^{1/2}$	1270 Gyr^{-1}	2286 Gyr^{-1}	B	Elmegreen (1994)
Instability growth rate	ω_r	1013 Gyr^{-1}	2206 Gyr^{-1}	B	

Note. — The Sun’s distance to the Galactic center is taken to be $R_{\odot} = 8$ kpc. The effective sound speed in the interstellar gas is c . Galactocentric radius is r . The column labeled “Accuracy” indicates the approximate errors — A: $\pm 20\%$; B: $\pm 50\%$; C: order-of-magnitude.

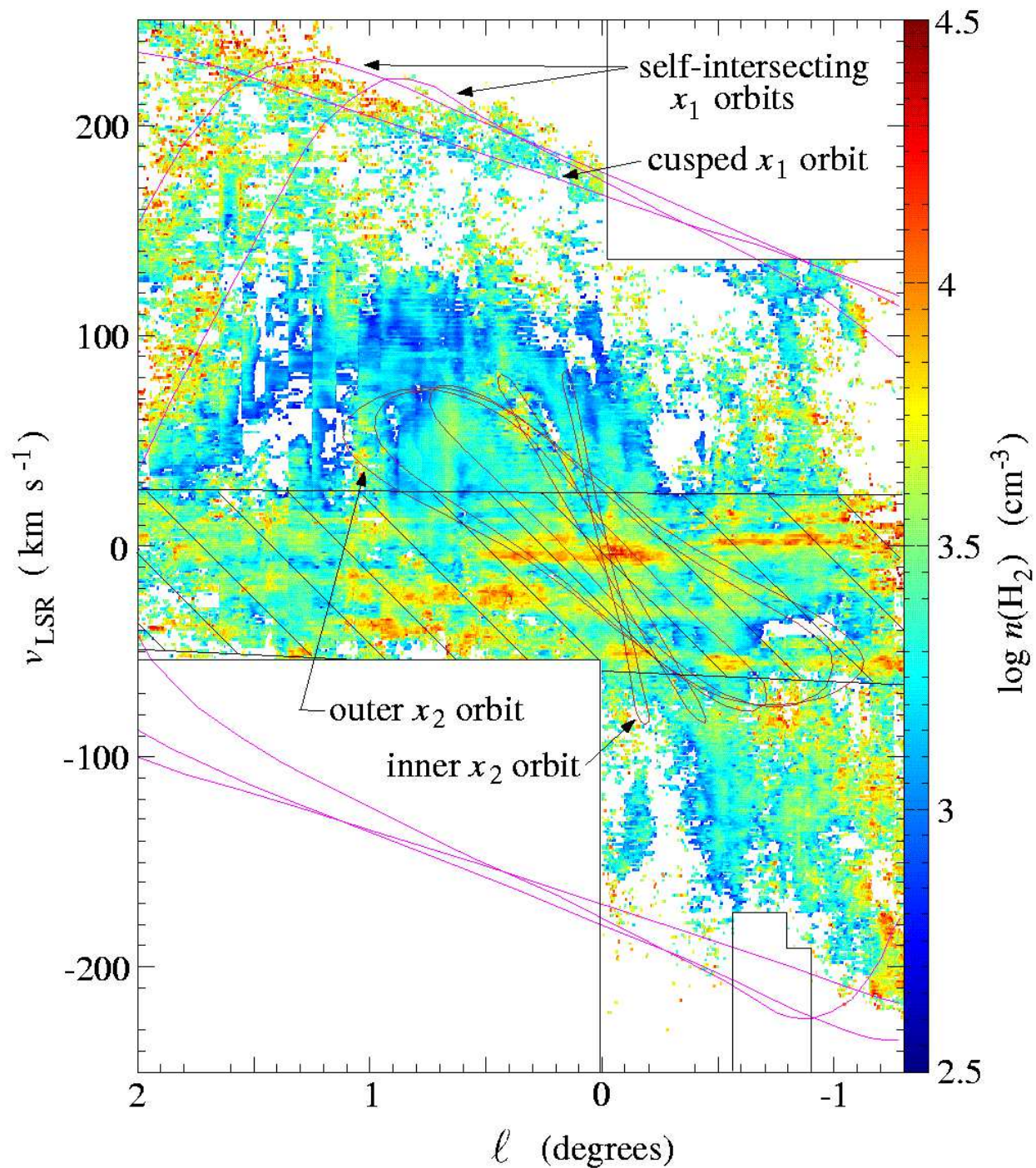


Fig. 1.— Density on x_1 and x_2 orbits in the inner Milky Way. The rainbow scale at right shows the average density of molecular gas from an LVG model using AST/RO survey data (Martin et al. 2004). White pixels are points where there are no data, or where the LVG model does not converge to consistent values. The hatched area at low velocity shows definite foreground absorption which invalidates the assumptions of the LVG model. Superposed on the density data are some x_1 (magenta) and x_2 (brown) orbits from Bissantz et al. (2003).